BIOCHEMISTRY
including biophysical chemistry & molecular biology
Article

Biochemistry **2010,** *49,* 1435–1447 1435
DOI: 10.1021/bi901783s

Localization of the Death Effector Domain of Fas-Associated Death Domain Protein into the Membrane of *Escherichia coli* Induces Reactive Oxygen Species-Involved Cell Death[†]

Nithyananda Thorenoor,[‡,⊥] Jin-Hee Lee,[§] Seong-Ki Lee,[§] Sung-Won Cho,[§] Yong-Hak Kim,[∥] Key-Sun Kim,[⊥,§] and Cheolju Lee*[,‡,⊥]

[‡]*Life Sciences Division, Korea Institute of Science and Technology, 39-1 Hawolgok, Seongbuk, Seoul 136-791, Korea,* [§]*Center for Neural Science, Korea Institute of Science and Technology, 39-1 Hawolgok, Seongbuk, Seoul 136-791, Korea,* [∥]*Functional Proteomics Center, Korea Institute of Science and Technology, 39-1 Hawolgok, Seongbuk, Seoul 136-791, Korea, and* [⊥]*University of Science and Technology, 52, Eoeun, Yuseong, Daejeon 305-333, Korea*

Received October 16, 2009; Revised Manuscript Received January 12, 2010

ABSTRACT: The death effector domain (DED) of the mammalian apoptosis mediator, Fas-associated death domain protein (FADD), induces *Escherichia coli* cell death under aerobic culture conditions, yet the mechanisms by which FADD-DED induces cell death are not fully understood. Oxidative stress has been implicated as one of the mechanisms. Using a proteomic approach and validation by coexpression analysis, we illustrate that overexpression of FADD-DED in *E. coli* invokes protein expression changes that facilitate conversion of pro-oxidant NADH into antioxidant NADPH. Typically, isocitrate dehydrogenase, phosphoenolpyruvate carboxykinase, and pyruvate kinase are downregulated and malate dehydrogenase is upregulated. We reasoned that such a change in *E. coli* cells is an active response to reduce the size of the NADH pool, thereby decreasing the level of ROS generation. From the coexpression studies, we observed that DNA binding protein Hns, which induces growth arrest when overexpressed heterologously, alleviated the cell killing effect of FADD-DED. FADD-DED was expressed as a noncovalently linked multimeric protein in the membrane of *E. coli*. Exogenous treatment of *E. coli* cells with FADD-DED in the presence of a membrane component induced cell death, which was accompanied by a shift of the redox balance and a decrease in the cellular ATP level. Cell death was blocked by prior expression of thioredoxin. Localization of FADD-DED to the membrane may shift the cells into a state that stimulates and fuels ROS generation. The cell death mechanism mediated by ROS may mimic antibiotic-mediated bacterial cell death or Bax-mediated apoptosis in mammalian cells. Our results provide a common mechanistic feature of ROS-involved cell death throughout prokaryotes and eukaryotes.

Apoptosis is a self-destructive process at work not only in multicellular higher eukaryotes but also in unicellular eukaryotic organisms and even in prokaryotic organisms (*1*−*4*). Apoptosis requires transmission of apoptotic signals and the involvement of pro-apoptotic molecules inside cells. Some mammalian molecules involved in apoptosis also affect the viability of bacterial cells. Bax is an example having such versatile activity (*5*), and the death effector domain (DEDs)[1] of the Fas-associated death domain protein (FADD) also induces bacterial cell death (*6*).

The FADD protein is a key adaptor molecule that transmits a death signal in mammalian cells. The protein consists of the N-terminal DED and C-terminal death domain (DD). The DED of FADD, originally described as protein−protein interaction domains involved in death receptor-initiated programmed cell death, has no enzymatic activity but rather acts as binding partner for other DEDs, thereby promoting the formation of protein complexes (*7*, *8*). In Fas-mediated apoptosis, FADD associates with Fas through DD and recruits procaspase-8 via DED, leading to activation of procaspase-8. Eventually, the cells die through subsequent activation of the caspase cascade accompanying cell shrinkage, chromatin condensation, and DNA fragmentation (*9*−*11*). In addition, apoptosis signals increase the cellular level of reactive oxygen species (ROS) by an unknown mechanism. Although DED-containing proteins are not found in bacteria, we previously reported that FADD-DED induced bacterial as well as mammalian cell death (*6*). *Escherichia coli* cells expressing FADD-DED exhibited elongated cell morphology and an increased level of nicked chromosomal DNA and mutation. This death effect is mysterious, because *E. coli* has no caspases or protein domains orthologous to those of the DED that mediate cell death in mammals. The lethality of FADD-DED in *E. coli* can be abolished by coexpression of thioredoxin (TrxA), suggesting that bacterial cell death may be induced by enhancing the cellular level of ROS (*6*). Since *E. coli* does not contain any effector molecule for apoptosis, more systematic

[†]This work was supported by grants from the Functional Proteomics Center (C.L.) and Microbial Genomics and Application Center (K.-S.K.).

*To whom correspondence should be addressed: Life Sciences Division, Korea Institute of Science and Technology, 39-1 Hawolgok, Seongbuk, Seoul 136-791, Korea. Tel: +82/(0)2/958-6788; Fax: +82/(0)2/958-6919; e-mail: clee270@kist.re.kr.

[1]Abbreviations: FADD, Fas-associated death domain protein; DED, death effector domain; DD, death domain; 2-DE, two-dimensional gel electrophoresis; CHCA, α-cyano-4-hydroxycinnamic acid; MALDI-TOF/TOF, matrix-assisted laser desorption ionization time-of-flight mass spectrometry; MS, mass spectrometry; MS/MS, tandem mass spectrometry; IDH, isocitrate dehydrogenase; MDH, malate dehydrogenase; PckA, phosphoenolpyruvate carboxykinase; PykF, pyruvate kinase; SDS−PAGE, sodium dodecyl sulfate−polyacrylamide gel electrophoresis.

Published on Web 01/13/2010

approaches are required for the elucidation of the bacterial cell death mechanism by mammalian FADD-DED.

Mass spectrometry (MS) used in combination with various protein separation methods and bioinformatics tools has become the routine method of proteomic research for identification and characterization of differentially expressed proteins in response to a certain physiological stimulus (*12*, *13*). Peptide mass fingerprinting is a simple and powerful technique for high-throughput protein identification (*14*, *15*). It can be applied more successfully when the genomes of aimed organisms are fully sequenced and annotated. *E. coli* has been frequently used as a model organism in structural and functional studies aimed at understanding bacterial physiology and gene expression, because the entire genome sequence of this organism is available (*16*). Therefore, applying proteomic methods in the study of *E. coli* proteins responding to the overexpression of FADD-DED will be a tractable approach in elucidating the mechanism of FADD-DED-mediated cell death.

In this study, we have elucidated the biological events during FADD-DED-induced cell death in *E. coli*. Through proteomic approaches together with coexpression studies, we show that expression of FADD-DED downregulates proteins involved in energy production and conversion, which is an active response of FADD-DED-expressing cells to overcome ROS effect. We present evidence of the localization of FADD-DED in the membranes, which brings an analogous inference to Bax-mediated apoptosis in mammalian cells where it targets the mitochondrial membrane. Our results indicate that FADD-DED-induced ROS generation is triggered by membrane localization of FADD-DED, which shifts the cells into a state that stimulates and fuels ROS and ultimately results in cell death. This phenomenon may mimic the mechanism observed in bactericidal antibiotic-induced cell killing. Our results elucidate a common mechanistic feature of ROS-dependent cell death throughout prokaryotes and eukaryotes.

EXPERIMENTAL PROCEDURES

Cell Growth and Protein Extraction. The pET3d-FADD-DED plasmid was cleaved with *Bgl*II and *Hin*dIII and transferred into the same sites of pET28a. As pET28a contains the lacI gene, the expression of FADD-DED is more tightly repressed in the absence of isopropyl β-D-galactopyranoside (IPTG) (*6*). *E. coli* BL21(DE3) pLysS cells harboring pET28a-FADD-DED were grown in Luria-Bertini (LB) medium containing kanamycin (50 μg/mL) and chloramphenicol (30 μg/mL). Cells were grown at 37 °C until the OD_{600} reached 0.5−0.6. To the exponentially grown culture was added 0.5 mM IPTG, and the culture was grown for a further 90 min at 37 °C to yield FADD-DED expression. The cells were then harvested by centrifugation at 1200*g* for 15 min. The harvested cells were washed with ice-cold water to remove excess culture medium present in the cells and stored frozen at −80 °C until they were required. Frozen cells were suspended in a 2-fold volume of solubilization solution containing 30 mM Tris (pH 8.5), 2 M thiourea, 7 M urea, and 4% CHAPS and disrupted by intermittent sonic oscillation. The unbroken cells and cellular debris were removed by centrifugation at 13200*g* for 60 min, and the supernatant was collected. The concentration of the protein preparation was determined by the Bradford method.

Two-Dimensional Gel Electrophoresis (*2-DE*). Isoelectric focusing (IEF) was performed by using a multiphor II IEF cell with a 24 cm ready strip at pH 4−7 (GE Healthcare, Uppsala, Sweden). Protein samples (400 μg in each) diluted in 80 μL of lysis buffer [30 mM Trizma base, 2 M thiourea, 7 M urea, 4% CHAPS, 0.2% DTT, and 1% IPG buffer (pH 4−7)] were loaded on IPG strips that had been previously rehydrated overnight. The IPG strips were focused at 20 °C, at a maximum voltage of 8000 V according to the following steps: S1, gradient to 500 V, over 2 h; S2, gradient to 1000 V, over 2 h; S3, gradient to 4000 V, over 2 h; S4, gradient to 8000 V, over 2 h; S5, constant at 8000 V, over 14 h. After IEF, the IPG strips were equilibrated in SDS equilibration buffer I [6 M urea, 30% glycerol, 2% SDS, 1% DTT, and 50 mM Trizma base (pH 8.8)] and then immediately treated with buffer II (1% DTT replaced with 2.5% iodoacetamide) for 15 min with constant shaking. The equilibrated strips were subjected to second-dimension separation on 12.5% SDS−polyacrylamide gels. Electrophoresis was conducted using a Hoefer DALT system (GE Healthcare) with a constant current (60 mA/gel) at 15 °C for approximately 6−7 h until the dye front reached the bottom of the gel. The gels were then fixed with 20% ethanol and 10% acetic acid and stained by the silver staining method (GE Healthcare).

Digitized images of silver-stained gels were generated by a Umax power look 2100XL scanner (Maxium Technologies, Taipei, Taiwan), and the image analysis was performed using Progenesis (www.nonlinear.com/2D). Protein spots were detected automatically, and manual spot editing was performed when necessary. The intensity of a protein was calculated by the spot volume integration by normalization of the individual spot volume versus the total spot volume in that gel. Only those protein spots for which the greatest alterations were more than 2-fold ($p < 0.05$) between control cells and FADD-DED-induced cells were selected for further characterization using mass spectrometry.

In Situ Digestion of Proteins and MALDI-TOF/TOF. Identification of differentially expressed protein spots was conducted as described previously (*17*, *18*). Silver-stained protein spots were excised from the gel and stain-stripped in 50 mM sodium thiosulfate and 15 mM potassium ferricyanide. Proteolytic peptides were recovered from the gel by an in-gel digestion method using 12.5 ng/μL sequencing-grade trypsin (Promega, Madison, WI) in 25 mM ammonium bicarbonate. Mass spectrometric analyses were performed using an AB 4700 Proteomics Analyzer (Applied Biosystems, Framingham, MA) in both MS and MS/MS modes. The mass spectrometer was set to acquire positive ion MS survey scans over the mass range of 700−3500 Da. Once the MS survey scans were completed, the data were processed to generate a list of precursor ions for interrogation by MS/MS. The instrument was equipped with a Nd:YAG laser (PowerChip, JDS Uniphase, San Jose, CA) operating at 200 Hz and controlled by Applied Biosystems Explorer version 1.1. The mass resolutions of the instrument were 15000 and 4000 in the MS and MS/MS modes, respectively. The mass accuracy in the MS mode was roughly ±30 ppm, while in the MS/MS mode, the mass accuracy was ±50 ppm. MS/MS was performed with air as the collision gas at a pressure of 1.4×10^{-6} Torr.

Protein identification was attempted by MS/MS ion search (mass tolerance for precursor ion, 100 ppm; fragment ion, 0.5 Da) on the basis of the TOF/TOF tandem mass spectrometric data from at least two peptides to interrogate the Swiss-Prot protein database (release 46.2, 176469 sequences) using Mascot (version 1.9, MatrixScience). Searches were performed to allow for a fixed modification of carbamidomethylation at cysteine and a maximum of one missed trypsin cleavage. The entire automatic data

analysis and database search were fulfilled by GPS Explorer (version 3.5, Applied Biosystems). Protein scores of greater than 75 were considered statistically significant ($p \leq 0.05$). If no reliable MS/MS spectrum was obtained (Mascot score of < 30), protein identification was attempted by peptide mass fingerprinting. For mass fingerprint analysis, each raw spectrum was opened in DataExplorer (version 4.6, Applied Biosystems) and fewer than 50 top mass peaks were selected by signal-to-noise threshold setting and then treated with advanced baseline correction and noise filter 0.7 functions. The spectrum was further calibrated with more than two peptides resulting from trypsin autolysis (m/z 842.5100, 1045.5642, 1940.9354, 2211.1046, 2283.1807, and 2807.3145). The filter peak list of monoisotopic masses was copied to the Mascot public interface and searched against the Swiss-Prot database (release 46.2, 176469 sequences) using the following parameters: trypsin as the enzyme, one possible missed cleavage, MH^+ monoisotopic masses, peptide tolerance of 30 ppm, and a fixed modification of carbamidomethylation at cysteine. A hit was considered to be significant if the scores obtained for PMF and MS/MS data clearly exceeded the significance threshold ($p \leq 0.05$).

Classification of Identified Proteins as Essential or Nonessential. The identified *E. coli* proteins were classified into essential and nonessential on the basis of the information obtained from the Profiling of *E. coli* Chromosome (PEC) database (www.shigen.nig.ac.jp/ecoli/pec/index.jsp), which classified genes as essential or nonessential on the basis of a combination of experimental evidence and general functional consideration. The genes for which null type mutants have been isolated are classified as "nonessential", and those for which conditional lethal mutants have isolated are classified as "essential" (*19*).

Coexpression of Differentially Expressed Proteins with FADD-DED. We used the pETduet1 expression vector (EMD Chemicals, Inc., Gibbstown, NJ) for coexpression studies, as this vector is designed for coexpression of two target genes under a single promoter. Among differentially expressed proteins in FADD-DED-induced *E. coli* cells, SlyD, Hns, DsdA, GatD, AtpC FabI, Pgk, Tsf, and RpsB were selected for the coexpression experiment and TrxA was included as a reference since its coexpression was effective in abolishing the lethal effect of FADD-DED (*6*). A DNA fragment of FADD-DED was obtained from the pET28a-FADD-DED plasmid via digestion with *Nco*I and *Bam*HI and subcloned into the first multiple cloning site (MCS I) of the pETduet1 plasmid, resulting in pETduet1-FADD-DED. A complete gene sequence encoding a selected protein was PCR amplified using genomic DNA of *E. coli* and ligated at the MCS II of pETduet1-FADD-DED by incorporation of compatible *Bgl*II and *Xho*I restriction sites at the ends of the PCR product for DsdA, or *Nde*I and *Bgl*II sites for the other genes. The PCR primers used are listed in Table S1 of the Supporting Information. The resultant dual gene expression vector was transformed into *E. coli* BL21(DE3) cells containing pLysS. The transformant was exponentially grown in LB medium at 37 °C and 200 rpm. If necessary, ampicilin (100 μg/mL) and chloramphenicol (30 μg/mL) were added to LB medium. When the OD_{600} reached 0.6−0.7, the two genes were simultaneously expressed by the addition of 0.5 mM IPTG, and the growth rates (OD_{600}) were measured.

Subfractionation of the Cell Extract and Purification of the FADD-DED Protein. The frozen cells were suspended in a 2-fold volume of solubilization solution containing 50 mM Tris-HCl (pH 7.3) and disrupted by intermittent sonic oscillation. The unbroken cells and cellular debris were removed by centrifugation at 13200*g* for 60 min. The supernatant (designated as "T") was collected and further centrifuged in a Beckmann 70 Ti rotor at 115000*g* for 1 h at 4 °C. The supernatant was collected (designated as "C"), and the pellet was resuspended and washed by using 50 mM Tris-HCl (pH 7.3), followed by ultracentrifugation at 115000*g* for 60 min at 4 °C. The resulting pellet (designated as "M") was resuspended in 50 mM Tris-HCl (pH 7.3). The "C" fraction was filtered through 3000 Da molecular mass cutoff (MWCO) filters (Millipore, Billerica, MA) to prepare small molecule material that passed through the filter membrane (designated as "F") and high-molecular mass substances retained in the upper part of the membrane (designated as "R"). The concentration of the protein preparation was determined by the BCA method. The cell extract preparations were checked via SDS−PAGE.

The FADD-DED protein was purified by ammonium sulfate precipitation followed by ion-exchange chromatography. The protein preparation obtained after the ultracentrifugation (M fraction) was precipitated via addition of 30% ammonium sulfate, with constant stirring at 4 °C for 45 min. The precipitated proteins were collected by centrifugation at 13200*g* for 15 min at 4 °C. The protein pellet was resuspended and washed using a 30% ammonium sulfate solution by gentle stirring, followed by centrifugation at 13200*g* for 15 min at 4 °C. The resulting pellet was resuspended in 50 mM Tris-HCl (pH 8.0) and recentrifuged at 13200*g* for 15 min at 4 °C to eliminate any precipitates. The supernatant was collected and applied on a DEAE-Sepharose column (GE Healthcare), which was equilibrated previously using 50 mM Tris-HCl (pH 8.0). After being washed, the proteins were eluted with a linear gradient from 0 to 0.6 M NaCl. The eluted protein fractions were dialyzed against 50 mM Tris-HCl (pH 8.0) by using 3500 MWCO dialysis sacks (Spectrum laboratories, Rancho Dominguez, CA) for 30 h. The dialyzed protein samples were concentrated by using 3000 MWCO ultra centrifugal filters (Millipore). The concentration of the protein preparation was determined by the BCA method. The purity of the resulting FADD-DED preparation was checked via SDS−PAGE by staining the gels with CBB R250.

Measurement of the Cytotoxic Effect of the Cell Extract and Purified FADD-DED Protein. *E. coli* BL21(DE3) cells were grown in LB medium at 37 °C until the OD_{600} reached 0.4−0.5, and the cells were serially diluted. The 100 μL cell samples from the 10^{-5} dilution were treated with 500 μg of purified FADD-DED protein or different subfractions of the cell extract prepared from *E. coli* cells which had overexpressed wild-type FADD-DED. The protein and cell mixture was incubated for 30 min and plated on LB-Agar. The plates were incubated at 37 °C overnight. The number of colonies that appeared on each agar plate was counted to estimate the cytotoxic effect of each protein sample on *E. coli*. The untreated 100 μL *E. coli* cell samples from the 10^{-5} dilution were used as a control.

Analytical Gel Filtration Chromatography. A Superdex-200 10/30 (GE Healthcare) column was used to determine the molecular mass of FADD-DED in the native state. The membrane extracts having FADD-DED proteins (1 mg/mL) were dissolved in 50 mM Tris-HCl buffer (pH 7.3) containing 0.15 M NaCl and 1% octyl β-glucoside. Samples were eluted at a flow rate of 0.25 mL/min, and 0.65 mL fractions per tube were collected. The fractions were analyzed via SDS−PAGE, and the gel was stained with CBB R250 following electrophoresis.

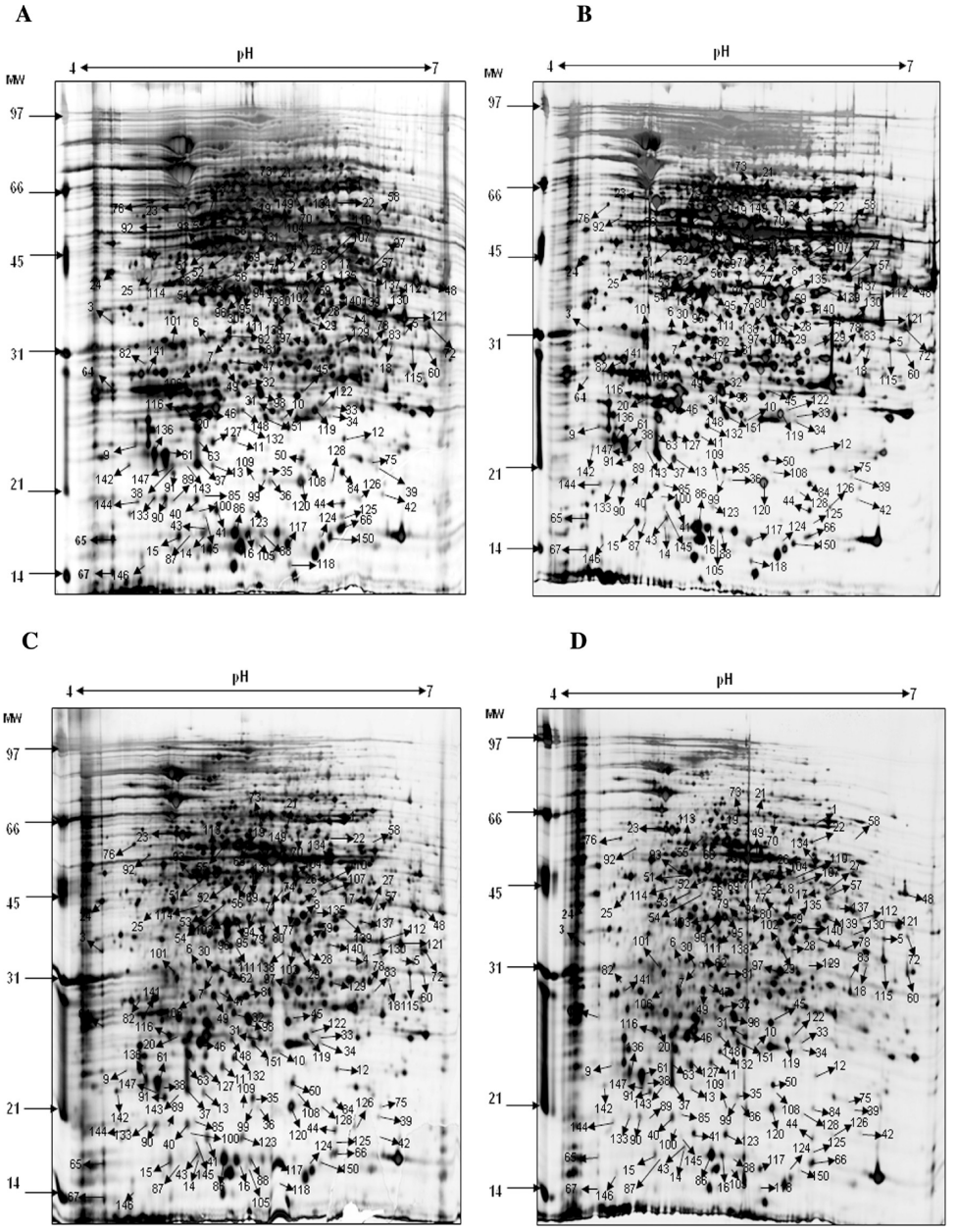

FIGURE 1: 2-DE patterns of *E. coli* cell proteins resulting from the expression of wild-type and mutant FADD-DED: wild type uninduced (A), wild type induced (B), mutant uninduced (C), and mutant induced (D). Differentially expressed proteins are indicated numerically, and the proteins identified by MALDI-TOF/TOF analysis are listed in Table S2 of the Supporting Information.

The intensity of the protein bands was quantified by using ImageQuant version 5.2 (GE Healthcare). The protein elution volume was compared with the elution volume of standard proteins. The following molecular mass standards were used: blue dextran (> 2000 kDa), β-amylase (200 kDa), alcohol dehydrogenase (150 kDa), BSA (66 kDa), carbonic anydrase (29 kDa), cytochrome *c* (12.4 kDa), and vitamin B_{12} (1.35 kDa).

Determination of Cellular Adenine Nucleotide Levels by High-Performance Liquid Chromatography (HPLC). *E. coli* BL21(DE3) cells were grown in LB medium at 37 °C and 180 rpm until the OD_{600} reached 0.5. Cells were harvested and washed with M9 medium. The washed cells were suspended in M9 medium to create an optical density of 5−10 and were equally dispensed into new containers with or without the addition of 500 μg/mL membrane FADD-DED (WIM), 40 μg/mL kanamycin, or 30 μg/mL polymyxin B. After incubation for 1 h at 37 °C and 180 rpm, the harvested cells were disrupted using 50 μL of lysis buffer containing 8 M urea and 1 mM DTT in 100 mM potassium phosphate buffer (pH 6.0) for 1 h on ice. Each sample was spiked with 0.5 mM 3-acetylpyridine adenine dinucleotide (acNAD) (Sigma, St. Louis, MO) as an internal standard to normalize elution times and peak areas of the analytes. The supernatant was collected after centrifugation at 13200*g* for 15 min and filtered through 3000 MWCO filters (Millipore). A 10 μL sample was injected via an Agilent (Santa Clara, CA) 1100 HPLC system into a Kromasil C_8 column (3.5 μm, 2 mm × 150 mm) (Phenomenex, Torrance, CA) and washed for 5 min with 100 mM potassium phosphate (pH 6.0), followed by a linear gradient of 0 to 5% methanol in the same buffer for 20 min at a flow rate of 0.25 mL/min. The internal standard acNAD eluted at 14.6 ± 0.1 min, and its normalized elution time (NET) was expressed as 1. Concentrations of ATP (net ± standard deviation, 0.179 ± 0.007), ADP (0.207 ± 0.006), AMP (0.324 ± 0.005), NADH (1.15 ± 0.020), NADPH (0.579 ± 0.003), NAD (0.476 ± 0.002),

and NADP (0.226 ± 0.007) were determined at 260 nm with a VWD detector. The standard curves were constructed using authentic chemicals with more than four data points in the range of a 5−50 nmol injection, which resulted in good linearity ($r^2 > 0.98$) and reproducibility (CV < 5%).

Statistical Analysis. We conducted statistical analysis with the Student's *t* test. We considered a *P* value of ≤0.05 as a significant difference.

RESULTS

Identification of Differentially Expressed Proteins in Response to FADD-DED. The proteomes from *E. coli* BL21-(DE3) pLysS cells that overexpressed FADD-DED were resolved by 2-DE (pH 4−7). The proteomes related to the cellular response to FADD-DED overexpression were characterized by pairwise comparisons among wild type uninduced, wild type induced, mutant uninduced, and mutant induced (the four systems are termed WU, WI, MU, and MI, respectively). The F25S mutant was selected as a control for proteomics study because it did not affect the growth, when compared to wild-type FADD-DED-expressing cells, where the *E. coli* cells stopped growing after the induction of protein. From the four gels, 929 (WU), 747 (WI), 1006 (MU), and 842 (MI) spots were detected. Of 151 protein spots that are differentially expressed in any one of the comparison sets by >2-fold (Figure 1), we successfully identified 82 proteins by mass spectrometry, and among them, a few spots resulted in identification of the same protein. A total of 73 proteins were finally identified and are listed in Table S2 of the Supporting Information.

The 73 identified proteins were classified into several groups according to their function, i.e., 19% of the identified proteins for energy production and conversion, 21% for amino acid transport and metabolism, and 11% for carbohydrate transport and metabolism such as glycolysis, gluconeogenesis, the TCA cycle, and fatty acid biosynthesis. Others were related to transcription (5%), translation (5%), post-translation modifications (7%), nucleotide transport and metabolism (3%), inorganic transport and metabolism (1%), and cell envelope biogenesis and outer membrane (8%), antioxidant (1%), and lipid metabolism (3%). We also identified some proteins whose function is not known yet (8%) (Figure 2A).

Thirty-five protein spots were identified as being differentially expressed by more than 2-fold in *E. coli* cells expressing wild-type FADD-DED compared to the F25S mutant [(WI/WU)/(MI/MU) ≥ 2, or (WI/WU)/(MI/MU) ≤ 0.5 (Table 1)]. Biological functions of these 35 proteins were diverse. Among them, proteins belonging to the functional group of energy production and conversion were more specifically enriched in the down-regulated protein set (Figure 2B and Table 1). The peptide sequences and scores are listed in Table S3 of the Supporting Information.

Inhibition of the Lethal Effect of FADD-DED by Co-expression of Differentially Expressed Proteins. To characterize the role of each individual protein that is up- or downregulated in response to the lethal effect of FADD-DED overexpression, we performed coexpression experiments by using a dual expression vector containing FADD-DED together with one of the proteins. We tested whether the lethality of FADD-DED is abolished by coexpression with the identified proteins. The target genes were selected by considering the difference between the ratio values of the wild type to mutant (WI/WU vs MI/MU); they were selected

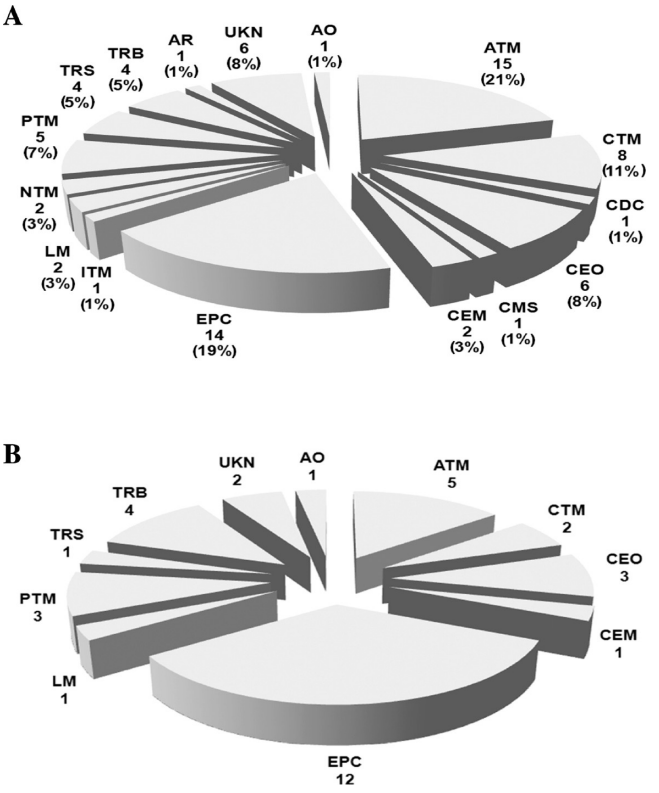

FIGURE 2: Functional classification of proteins identified from *E. coli* cells expressing FADD-DED. (A) The 73 identified proteins are classified into subgroups according to their function. Gene ontology data used for functional annotation were retrieved from NCBI COGs (http://www.ncbi.nlm.nih.gov/COG/). (B) Of 73 proteins, 35 exhibiting a >2-fold difference are classified according to their function. Protein function codes: ATM, amino acid transport and metabolism; CTM, carbohydrate transport and metabolism; CDC, cell division and chromosome partitioning; CEO, cell envelope biogenesis, outer membrane; CMS, cell motility and secretion; CEM, coenzyme metabolism; EPC, energy production and conversion; ITM, inorganic ion transport and metabolism; LM, lipid metabolism; NTM, nucleotide transport and metabolism; PTM, post-translational modification; TRS, transcription; TRB, translation, ribosome structure, and biogenesis; AR, antibacterial resistance; UKN, unknown; AO, antioxidant.

if the ratio between the two values is greater than 5 or less than 0.2. The subset protein list is summarized in Table S4 of the Supporting Information. The TrxA is used as a control in the coexpression studies. TrxA is known to control the cellular redox potential by formation of a disulfide bond between two cysteines located in the active site, and this protein was characterized to abolish the lethal effect of FADD-DED (*6*).

The coexpression of SlyD and Hns resulted in better growth than in the cells expressing DED alone and the cells coexpressing TrxA (Figure 3 and Table S4 of the Supporting Information). The *E. coli* cells coexpressing D-serine dehydratase (DsdA), galactitol-1-phosphate 5-dehydrogenase (GatD), phosphoglycerate kinase (Pgk), elongation factor TS (Tsf), and enoyl-[acyl carrier protein] reductase (FabI) had better cell growth than the DED-expressing cells, but the growth rate was similar to that of TrxA-coexpressing cells (Figure 3 and Table S4 of the Supporting Information). The *E. coli* cells coexpressing the ATP synthase ε-chain (AtpC) and 30S ribosomal protein S2 (RpsB) were not significantly different from the cells expressing FADD-DED alone, so they appeared not to be beneficial against FADD-DED in *E. coli*.

Table 1: Proteins Differentially Expressed in *E. coli* Cells Expressing FADD-DED and Identified by MALDI-TOF/TOF

spot	accession number[a]	protein name	fold change[b] WI/WU	fold change[b] MI/MU	cellular location[c]	function[d]
		Upregulated Proteins in Wild-Type FADD-DED-Expressing *E. coli* Cells				
7	P17994	uncharacterized protein yfaA	2.66	1.11	U	UKN
8	P61891	malate dehydrogenase	2.16	0.88	C	EPC
18	P0A6L2	dihydrodipicolinate synthase	2.66	0.92	C	ATM
43	P0A917	outer membrane protein X precursor	6.70	3.10	OM	CEO
45	P0A910	outer membrane protein A precursor	3.36	1.34	OM	CEO
66	P0A7R1	50S ribosomal protein L9	2.08	0.56	C	TRB
131	P00926	D-serine dehydratase	2.84	0.00	C	ATM
		Relatively Upregulated Proteins in Wild-Type FADD-DED-Expressing *E. coli* Cells				
4	P0AB77	2-amino-3-ketobutyrate coenzyme A ligase	1.90	0.67	C	CEM
79	P61891	malate dehydrogenase	1.08	0.38	C	EPC
86	P0A862	thiol peroxidase	1.87	0.49	P	AO
88	P69828	PTS system galactitol-specific IIA component	1.04	0.44	C	CTM
117	P0ACF8	DNA-binding protein H-NS (histone-like protein HLP-II)	0.73	0.00	C	TRS
118	P0A6E6	ATP synthase ε-chain	0.95	0.00	IM	EPC
129	P0AEK4	enoyl-[acyl carrier protein] reductase	1.03	0.00	C	LM
		Downregulated Proteins in Wild-Type FADD-DED-Expressing *E. coli* Cells				
11	P0AFP6	hypothetical UPF0135 protein ybgI	0.43	0.97	U	UKN
17	Q8XA55	serine hydroxymethyltransferase	0.40	1.41	C	ATM
21	P22259	phosphoenolpyruvate carboxykinase	0.41	1.02	C	EPC
27	P0A9S3	galactitol-1-phosphate 5-dehydrogenase	0.07	0.49	C	EPC
60	P0A7V0	30S ribosomal protein S2	0.00	0.75	C	TRB
62	P0A6P1	elongation factor TS	0.00	1.00	C	TRB
68	P0A6H5	ATP-dependent hsl protease ATP-binding subunit hslU	0.49	1.99	C	PTM
69	P0A836	succinyl-CoA synthetase β-chain	0.50	1.45	C	EPC
70	P37191	putative tagatose 6-phosphate kinase gatZ	0.24	1.10	C	CTM
74	P0A9S3	galactitol-1-phosphate 5-dehydrogenase	0.00	0.33	C	EPC
106	P0A9K9	FKBP-type peptidyl-prolyl *cis*/*trans* isomerase slyD	0.00	0.33	C	PTM
		Relatively Downregulated Proteins in Wild-Type FADD-DED-Expressing *E. coli* Cells				
1	P0AD61	pyruvate kinase I	0.58	1.58	C	EPC
16	P02358	30S ribosomal protein S6	0.76	1.63	C	TRB
71	P27248	aminomethyltransferase	0.82	2.89	C	ATM
76	P0ABB0	ATP synthase α-chain	1.01	3.04	IM	EPC
92	P0A6E4	argininosuccinate synthase	1.13	2.53	C	ATM
93	P08200	isocitrate dehydrogenase	0.85	2.17	C	EPC
107	Q8X9J9	UDP-*N*-acetylglucosamine 1-carboxyvinyltransferase	0.68	2.49	C	CEO
111	P0A799	phosphoglycerate kinase	0.83	4.16	C	EPC
113	P0A850	trigger factor	1.13	3.40	C	PTM
114	P0ABB4	ATP synthase β-chain	1.44	3.25	IM	EPC

[a]Accession number for the Swiss-Prot protein database. [b]Fold change in *E. coli* cells expressing wild-type and mutant DED. [c]Cellular location code: C, cytoplasm; IM, inner membrane; OM, outer membrane; P, periplasm; U, unknown. [d]Protein function code: TRS, transcription; EPC, energy production and conversion; ATM, amino acid transport and metabolism; CEO, cell envelope biogenesis, outer membrane; TRB, translation, ribosome structure, and biogenesis; UKN, unknown; PTM, post-translational modification; CTM, carbohydrate transport and metabolism; LM, lipid metabolism; CEM, coenzyme metabolism; AO, antioxidant.

We performed SDS−PAGE analyses of the transformants to confirm actual expression of the target proteins in the coexpression system. Distinct protein bands corresponding to the molecular masses of the selected target proteins as well as FADD-DED were detected via SDS−PAGE (Figure S1 of the Supporting Information). Therefore, the insignificant effect of AtpC and RpsB could not be attributed to the lower expression level but to the nature of the proteins. The essentiality of the genes for cell survival did not appear to correlate with the beneficial effect on the growth of the FADD-DED-expressing cells. The coexpression studies resulted in similar counts of essential and nonessential genes which were effective against FADD-DED in *E. coli*. Moreover, both Hns and SlyD, which were most effective in abolishing FADD-DED activity, were categorized as nonessential genes (*19*).

Membrane Localization of the FADD-DED Protein. The observation made with the comparative proteomic approach, in which proteins involved in energy production and conversion were significantly affected by FADD-DED expression, brought an analogous inference to Bax-mediated apoptosis in mammalian cells, which prompted us to investigate the localization of FADD-DED in *E. coli*. The cell extracts from *E. coli* cells expressing FADD-DED (WI) were separated according to the experimental design shown in Figure 4A and analyzed by SDS−PAGE. After the cells were induced for the expression of FADD-DED, a thick band at ~10 kDa appeared (Figure 4B,

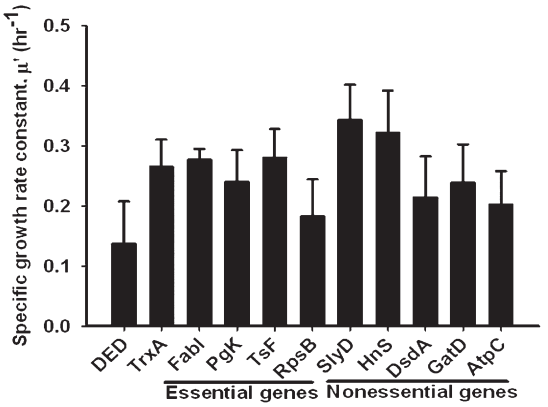

FIGURE 3: Specific growth rate of *E. coli* cells expressing FADD-DED alone or along with *trxA* or each of the selected genes. The selected target genes were coexpressed with FADD-DED in a dual expression system, and cell growth was measured via OD_{600}. DED denotes expression of FADD-DED alone as a negative control. TrxA denotes a positive control coexpressing TrxA as an effective gene that is able to abolish the lethal effect of FADD-DED. The bar size and error bar are the estimated means of specific growth rate constants and standard errors of the estimated means, respectively, which are determined from nonlinear regression of the exponential growth curve after the IPTG induction of active gene product(s).

T of WI), which was identified as the FADD-DED protein by in-gel trypsin digestion and mass spectrometry analysis. Interestingly, the FADD-DED protein was precipitated by ultracentrifugation at 115000*g* (M). Other proteins precipitated at this speed were all identified as membrane proteins such as outer membrane protein LamB, OmpF, MipA, etc. (in Figure 4B, identified proteins are listed below the gel image), suggesting membrane localization of the FADD-DED protein. The identification of FADD-DED as a membrane protein by mass spectrometry analysis was further supported by immunobloting observation with the anti-human FADD mouse antibody (data not shown). In the case of the F25S mutant, FADD-DED was not identified from the membrane fraction but was identified from the supernatant fraction of the ultracentrifugation step (Figure 4B, C of MI), which could be attributed to the cytosolic fraction because some representative thick bands corresponded to cytosolic proteins (data not shown). These data altogether suggest that the cytotoxic effect of FADD-DED is associated with its ability to localize in the membranes.

To determine the molecular mass of the FADD-DED protein in native state, gel filtration chromatography was exploited in a buffer containing 1% octyl β-glucoside. When the membrane fraction (M of WI) was loaded onto the column, the FADD-DED protein band was observed in a wide range of eluted fractions. Via comparison of the elution volume to those of standard proteins, the molecular mass of FADD-DED under native conditions was estimated to be between 66 and 200 kDa (Figure 4C). The chromatographic pattern did not change even in the absence of octyl β-glucoside (data not shown). These observations suggest that membrane-expressed FADD-DED in *E. coli* does not behave as a monomeric protein. Rather, its behavior is consistent with it being a noncovalently linked multimeric protein.

The Membrane FADD-DED Protein Induces Cell Death in E. coli. Since the overexpression of FADD-DED inside cells induces cell death, we next tested whether there are some endogenous messengers mediating the signal from the overexpressed FADD-DED protein or whether addition of the FADD-DED protein to the cells from outside also induces cell death. Cell extracts of FADD-DED-overexpressing cells were separated according to the scheme depicted in Figure 4A, and normal *E. coli* BL21(DE3) cells without the FADD-DED overexpression vector were treated with each separated fraction. The treated cells were spread on an agar plate and grown overnight, and the colonies were counted. By comparing the number of colonies, we could evaluate the cytotoxic effect of each fraction. Treatment with total cell extract (T) brought about a small decrease in colony count ($P < 0.01$). However, neither cytosolic fraction (C), its small molecule filtrate through ultracentrifugal filters (F), nor the retained high-molecular mass substances in the upper part of the membrane (R) exhibited any significant effect. The cytotoxic effect mainly resided in the membrane fraction. *E. coli* cells treated with the membrane extract having FADD-DED (M) exhibited a significant reduction in colony count ($P < 0.001$) relative to *E. coli* cells treated with other fractions (Figure 5A). It is likely that the protein itself exerts a cell killing effect even when it is added exogenously, and possible messengers may not be accumulated inside cells.

We next purified FADD-DED from the membrane fraction to electrophoretic homogeneity by using ammonium sulfate fractionation and ion-exchange chromatography (Figure 5B). Unexpectedly, when *E. coli* cells were treated with the purified FADD-DED proteins, there was no significant effect on cell survival and the number of colonies was quite similar to that seen with untreated *E. coli* cells or the cells treated with membrane fractions of uninduced cells (WUM). This demonstrates that the increase in the level of cell death is specific to the action mechanisms of FADD-DED proteins anchored in membranes. Similarly, treatment of *E. coli* cells with mixed protein samples, that is, purified FADD-DED mixed with membrane extracts of uninduced cells (WUM), restored the efficacy of cell killing [$P < 0.001$ (Figure 5B)].

To determine whether the cell death in *E. coli* treated with membrane-anchored FADD-DED involves the induction of an oxidative response, we examined the cell killing efficacy of the membrane FADD-DED protein on TrxA-expressing cells. We chose to examine TrxA-expressing cells because TrxA proteins significantly abolished the cell killing efficacy of FADD-DED when it is coexpressed (Figure 3). The TrxA-expressing *E. coli* cells were treated with membrane FADD-DED proteins. We found that TrxA protected the cells from FADD-DED-induced cell death [$P < 0.001$ (Figure 5C)]. These data reveal that cell death induced by the membrane-localized FADD-DED protein in *E. coli* involves ROS, whether it is overexpressed or added to the cells from the outside.

The cellular level of adenine nucleotides was determined for the *E. coli* cells treated with membrane FADD-DED (WIM). When compared to untreated cells, the treated cells displayed a sharp decrease in the ATP level relative to the total adenylate concentration, i.e., [ATP] + [ADP] + [AMP] and an increase in the redox balance expressed as ($[NAD^+][NADPH]$)/($[NADH]$-$[NADP^+]$) (Table 2). The WIM-treated cells accumulated NADPH significantly but had lowered concentrations of NADP and ATP versus those in the untreated cells. However, no significant change in redox balance and ATP level was observed in kanamycin-treated cells, but in the case of polymyxin B-treated cells, there was an increase in redox balance but the ATP level remained similar to that of untreated cells (Table 2). The decreased ATP level in the *E. coli* cells treated with membrane FADD-DED indicates a shift in the cellular energy level under ROS stress.

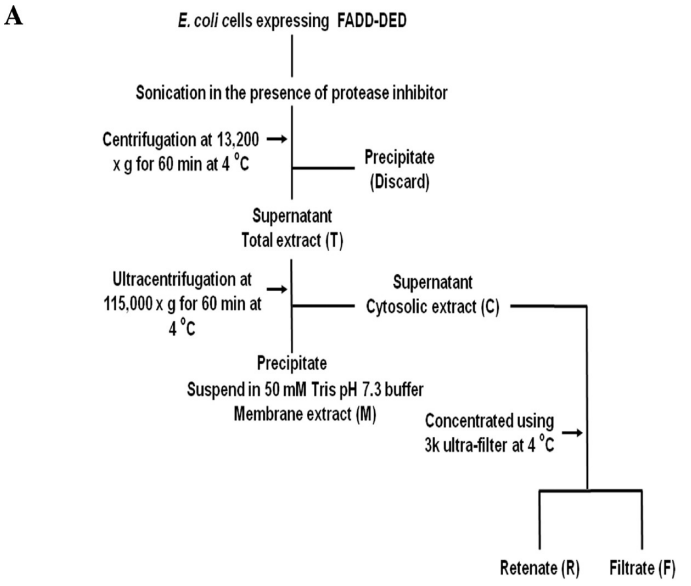

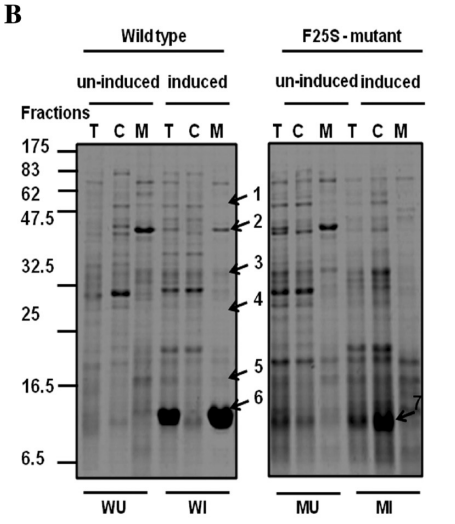

Band No.	Gene Name	Cellular location
1	LamB	Outer membrane
2	OmpF	Outer membrane
3	OmpA	Outer membrane
4	MipA	Outer membrane
5	OmpX	Outer membrane
6	FadD	Membrane of WI cells
7	FadD	Cytosol of MI cells

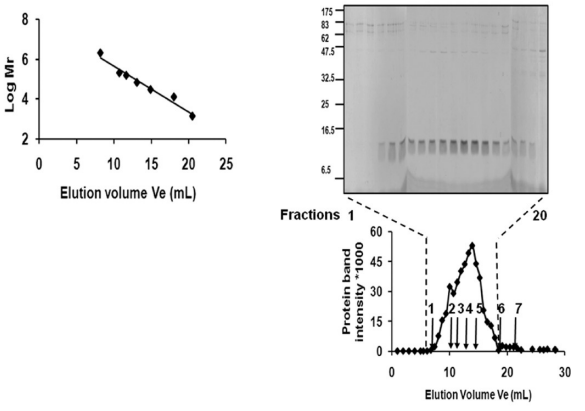

FIGURE 4: (A) Schematic representation of the experimental procedure for fractionation of cell extracts from FADD-DED expressed in *E. coli*. (B) The fractions were prepared from the wild type uninduced (WU), wild type induced (WI), F25S uninduced (MU), and F25S induced (MI). *E. coli* cells were analyzed by SDS−PAGE and visualized by CBB staining. Protein bands selected for identification (WIM) are denoted with an arrow. Identified proteins are listed below the gel image: LamB, maltoporin; OmpF, outer membrane protein F; OmpA, outer membrane protein A; MipA, Mlta-interacting protein; OmpX, outer membrane protein X; FadD, FADD-DED. (C) Gel filtration chromatography of FADD-DED. Membrane fractions of *E. coli* cells expressing FADD-DED (WIM) were separated using a Superdex-200 column in the presence of 1% octyl β-glucoside. The FADD-DED protein band was observed in a wide range of eluted fractions. The column was calibrated with protein standards. The following protein standards were used: (1) blue dextran (> 2000 kDa), (2) β-amylase (200 kDa), (3) alcohol dehydrogenase (150 kDa), (4) BSA (66 kDa), (5) carbonic anydrase (29 kDa), (6) cytochrome *c* (12.4 kDa), and (7) vitamin B_{12} (1.35 kDa).

DISCUSSION

In this study, we focused on the FADD-DED protein and its cell death mechanism in *E. coli* cells. Differentially expressed proteins in response to FADD-DED-induced bacterial cell death were discovered by a proteomic approach. We observed that proteins involved in energy production and conversion were significantly affected by FADD-DED overexpression and they were mostly downregulated. These observations prompted us to investigate the localization of FADD-DED inside the cells because the cell death process is similar to Bax-mediated apoptosis in mammalian cells. We detected constitutive expression of FADD-DED in the membranes of *E. coli* cells, and this membrane localization is critical to the cytotoxic effect of FADD-DED.

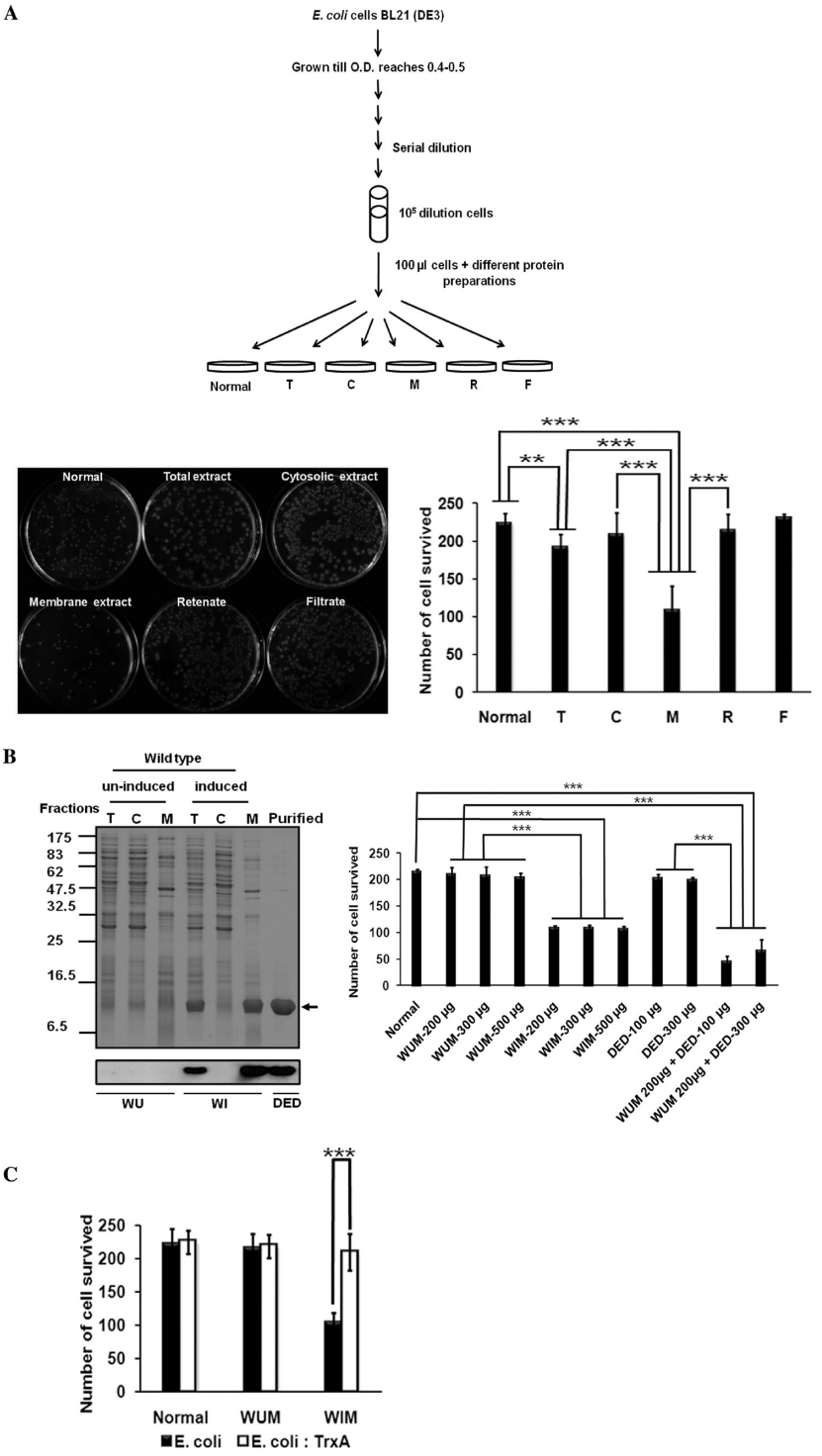

FIGURE 5: Cytotoxic effect of the FADD-DED protein on bacterial growth. (A) Schematic representation of the experimental procedure for *E. coli* cells treated with different protein preparations. The effect of cell extracts isolated from wild type FADD-DED-expressing cells on the viability of normal *E. coli*. The *E. coli* BL21(DE3) cells that had been grown exponentially in LB medium were diluted, and 100 μL of a 10^{-5} dilution of cells was treated with 500 μg protein samples from total extract (T), cytosolic extract (C), membrane extract (M), and retenate (R) and 250 μL from filtrate (F) and spread on LB plates. In the case of the filtrate, the protein concentration was very low; therefore, cells were treated with the same volume equivalent to that of the cytosolic extract. All the plates were incubated at 37 °C. The number of colonies was counted and is represented by bar graphs. Values were expressed as means ± standard deviation of three independent experiments performed in duplicate. Statistical significance (***$P < 0.001$; **$P < 0.01$) was analyzed by a Student's *t* test as indicated. (B) Effect of the purified FADD-DED protein on cell viability. The FADD-DED protein was purified from membrane extracts of FADD-DED-induced *E. coli* cells. After SDS−PAGE, gels were stained with CBB R250 (top) or analyzed by Western blot (bottom). Each lane was loaded with an equal amount of total protein (5 μg). The arrow indicates the FADD-DED protein. Various amounts of purified FADD-DED were mixed with membrane fractions of uninduced *E. coli* cells (WUM). The cytotoxic effect of each mixture was tested as described. Values are expressed as means ± standard deviation of three independent experiments performed in duplicate. Statistical significance (***$P < 0.001$) was analyzed by a Student's *t* test as indicated. (C) Cytotoxic effect of membrane FADD-DED reversed by thioredoxin. TrxA-expressed *E. coli* cells were treated with 500 μg of membranous FADD-DED (WIM). *E. coli* cells treated with WUM and untreated *E. coli* cells were used as controls. Values are expressed as means ± standard deviation of three independent experiments performed in duplicate. Statistical significance (***$P < 0.001$) was analyzed by a Student's *t* test as indicated.

Table 2: Measurement of Adenine Nucleotides in *E. coli* BL21(DE3) Cells after Treatment with Membrane FADD-DED and Antibiotics

	concentration (nmol/10^9 cells)								
test[a]	ATP	ADP	AMP	NAD	NADP	NADH	NADPH	ATP level[b]	redox balance[c]
control (untreated cells)	9.1 ± 2.2	5.4 ± 0.8	2.5 ± 0.1	4.7 ± 0.3	7 ± 0.3	0.27 ± 0.1	12.3 ± 2.7	0.53	30.3
kanamycin (40 μg/mL)	7.7 ± 1.3	4.8 ± 0.8	2.5 ± 0.4	3.1 ± 1.5	5.7 ± 0.3	0.18 ± 0.1	11.0 ± 1.4	0.51	33.2
polymyxin B (30 μg/mL)	10.9 ± 2.3	6 ± 0.9	1.9 ± 0.4	5.8 ± 1.7	10.2 ± 1.6	0.19 ± 0.1	12.9 ± 1.5	0.58	38.7
membrane FADD-DED (WIM, 500 μg/mL)	5.1 ± 1.4	4.7 ± 2.2	1.9 ± 0.4	3.3 ± 1.0	3.7 ± 0.6	0.13 ± 0.1	8.2 ± 1.3	0.43	54

[a]Values expressed as means ± standard deviation of independent experiments. [b]ATP level = [ATP]/([ATP] + [ADP] + [AMP]). [c]Redox balance = ([NAD][NADPH])/([NADH][NADP]).

The full-length FADD's subcellular location is confined to the cytoplasm and nucleus in mammalian cells (*20*), and DED of FADD is known as a protein−protein interaction domain without any enzymatic activity (*7*, *8*). Membrane localization of the FADD protein in mammalian cells has not yet been demonstrated. The cell death effect observed in our experiment by overexpression of FADD-DED in *E. coli* cells or by treatment of normal *E. coli* cells with the purified FADD-DED protein in the presence of a membrane component is due to the localization of the protein to the cell membrane. This was further supported by the observation made in the nonlethal variant F25S mutant where it could not localize in the membrane but mainly found in the cytosolic fraction. The localization of FADD-DED in the membrane might have activated the respiratory chain by a hitherto unknown mechanism, leading to enhanced ROS formation. ROS, including hydrogen peroxide and hydroxyl radical, are known to cause damage to proteins and membranes and increased levels of DNA damage and mutation (*21*, *22*). Consistent with this, increases in the level of nicked DNA and mutation were observed in FADD-DED-overexpressing cells (*6*). The phenomenon of cell death may mimic the mechanism observed recently by Kohanski et al. (*23*), who demonstrated that the changes in membrane integrity and hydroxyl radical formation are mainly related to bactericidal antibiotic-mediated *E. coli* cell death.

ROS are mostly generated from the energy production pathway when the cells are grown in an aerobic environment. To overcome the harmful effects of ROS, cells need to be equipped with various antioxidant enzymes (*24*). Peroxidases, catalases, and superoxide dismutases are among the critical enzymes that are utilized to keep ROS in check. In this study, an antioxidant enzyme, thiol peroxidase (Tpx), which resides in the periplasmic space of *E. coli* (*25*) was upregulated in *E. coli* cells expressing FADD-DED. Upregulation of Tpx is likely an active response against oxidative stress induced by FADD-DED overexpression. It was shown that, when *E. coli* cells are treated with oxidative stress-inducing reagents, the viability of individual Tpx mutant cells was much lower than that of wild-type cells (*26*).

The biological functions of antioxidant enzymes depend on the cellular level of reduced nicotinamide dinucleotide phosphate (NADPH) (*27*). The metabolic modules normally associated with glycolysis, gluconeogenesis, the TCA cycle, and glyoxylate cycle coalesce to create a unique network for the transfer of hydrogen from NADH to NADPH (*28*). The data in this study point to a metabolic network dedicated to the conversion of NADH into NADPH in *E. coli* as a consequence of oxidative stress. NADPH is central to any antioxidant defense strategies in an organism as it is the ultimate power that fuels the reductive cellular processes. Recently, it was shown that during bacterial cell death induced by bactericidal antibiotics NADH is utilized to generate ROS (*29*, *30*). The observation of changes in the cellular redox balance and ATP level in the FADD-DED-treated cells was well correlated with our proteomic observation in which MDH was upregulated and pyruvate kinase (PykF) and phosphoenolpyruvate carboxykinase (PckA) were downregulated in *E. coli* cells expressing FADD-DED (Figure 6A). In this instance, enzymes involved in disparate metabolic pathways seemingly partner to create a metabolic network aimed at converting NADH into NADPH. The malate is converted into pyruvate by the malic enzyme (MaeB), generating NADPH (*31*). Pyruvate is then subsequently converted back into malate with the aid of phosphoenolpyruvate synthase (PpsA), phosphoenolpyruvate carboxylase (Ppc), and MDH. This process requires the oxidation of NADH and hydrolysis of ATP. The downregulation of PckA and PykF would ensure that oxaloacetate is funneled toward malate production. The conversion of pyruvate to oxaloacetate and participation of NADH may provide an effective metabolic module for generating NADPH during oxidative stress (Figure 6B). An increase in the pool of NADPH in *E. coli* cells expressing FADD-DED will help to overcome the consequences of oxidative stress.

The NADH, generated from NAD during the TCA cycle, is key in causing out ROS-mediated cell death in bacteria. The fact that the toxicity of FADD-DED occurs only under aerobic culture conditions is intimately associated with ROS generation, since it is prevented under anaerobic conditions (*6*). The downregulation of isocitrate dehydrogenase (IDH) and succinyl-CoA synthetase β-chain expression in FADD-DED-expressing *E. coli* cells will reduce the size of the available pool of NADH which in turn decreases the level of ROS generation and leads to greater cell survival. More recently, Kohanski et al. (*29*) demonstrated that the loss of IDH led to a large increase in the survival rate after the exposure of bacteria to bactericidal drugs. They suggested that a decrease in the rate of survival was closely correlated to the number of NADH molecules produced, since NADH is produced at different points along the TCA cycle. The ATP concentration of a cell is an important determinant of survival or death (*32*). The level of ATP synthesis may decrease in *E. coli* cells expressing wild-type FADD-DED, as NADH plays an important role in the production of ATP during different steps of the electron transport system. It is ambivalent that the decrease in the level of NADH reduces the level of ATP production but protects the cell from the oxidative damage. The upregulation of outer membrane proteins, OmpA and OmpX, by FADD-DED-induced cells will open more passage of the essential nutrients that are needed to survive at low NADH and ATP levels.

The coexpression studies made more evident the fact that upregulated proteins are able to counteract FADD-DED, except for AtpC. The efficacies of DsdA (amino acid metabolism) and

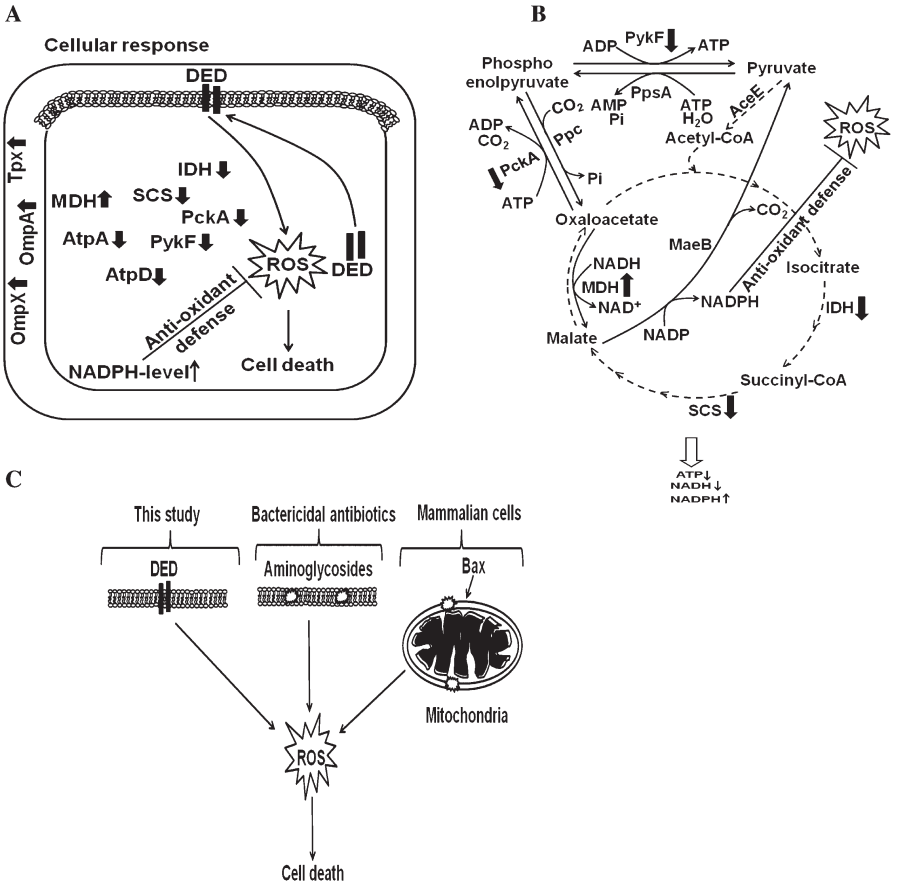

FIGURE 6: Schematic illustration of ROS generation by FADD-DED and antioxidant defense strategy. (A) Cellular response to FADD-DED-induced cell death. Overexpression of FADD-DED in the membranes of *E. coli* results in generation of ROS and cell death. Differential expression of proteins involved in the TCA cycle results in generation of an antioxidant NADPH from pro-oxidant NADH to protect the cells from oxidative damage. The large black arrows indicate up- and downregulated proteins in our study. (B) Proposed model for the cellular defense mechanism for overcoming oxidative stress. The conversion of NADH into NADPH and the reduced level of generation of NADH in various steps of the TCA cycle will help *E. coli* cells actively defend against ROS: PykF, pyruvate kinase; AceE, pyruvate dehydrogenase; PckA, phosphoenolpyruvate carboxykinase; PpsA, phosphoenolpyruvate synthase; Ppc, phosphoenolpyruvate carboxylase; IDH, isocitrate dehydrogenase; SCS, succinyl-CoA synthetase subunit; MDH, malate dehydrogenase; MaeB, NADP-linked malic enzyme. The large black arrows indicate up- and downregulated proteins in our study. (C) Common mechanism of cell death in prokaryotic and eukaryotic organisms. The generation of ROS by localization of FADD-DED in the membrane resembles antibiotic-mediated cell death in *E. coli* as well as Bax-mediated apoptosis in eukaryotes.

FabI (lipid metabolism) against FADD-DED are similar to that of TrxA, which moderately reduces the lethal effect of FADD-DED (*6*). Among the upregulated proteins tested for coexpression, Hns is the most efficacious against FADD-DED. It is a histone-like protein that binds tightly to DNA and strongly represses the expression of several genes (*33*). Heterologous overexpression of the Hns protein in exponentially growing *E. coli* caused silencing of global transcription, leading to a prolonged period of holding in which cells are viable but unable to grow (*34*). It is similar to a silent information regulator (SIR) gene in yeasts (*35*). In contrast, Hns overexpression induced better cell growth in the FADD-DED background. It is noteworthy that the life span of growth-arrested *E. coli* cells can be significantly extended via the omission of oxygen, and a significant number of genes induced by stasis are intimately associated with the protection against endogenously generated oxidative damage (*36*, *37*). Likewise, the cell killing activity of FADD-DED is more effective in the actively growing cells, and global suppression of transcription by Hns supports better adaptation to the stress induced by FADD-DED.

Overexpression of even some downregulated proteins, including GatD, Pgk, SlyD, and Tsf, enabled better growth of *E. coli* cells than FADD-DED alone. Among them, SlyD was most effective in abolishing the lethal effect of FADD-DED and much better than TrxA. It is a putative folding helper protein with the properties of prolyl isomerase and chaperone (*38*). However, it is uncertain how the FADD-DED-producing strain downregulates those effective proteins that can counteract FADD-DED. It is probable that the proteins may not be directly regulated by FADD-DED but serve as downstream targets for the toxicity of FADD-DED. Another possibility is that during FADD-DED-mediated cell death the proteins undergo post-translational modification, which changes their pI and molecular mass on 2-DE resulting in decreased spot intensity at the original position. In fact, a number of proteins are significantly modified by ROS at their cysteine, methionine, or tryptophan residues, leading to changes in their physicochemical properties for gel separation (*39*−*41*). These effective but downregulated proteins against FADD-DED deserve further study in an attempt to unveil genetic mechanisms or interactions with other important factors that are related to cell survival and growth under oxidative stress.

The cell death caused by the overexpression of FADD-DED in membranes of *E. coli* resembles Bax-induced cell death in mammalian, yeast, and *E. coli* cells (*5*, *42*−*45*). Bax is a 21 kDa

pro-apoptotic membrane protein with a membrane anchor sequence at the C-terminus and promotes apoptosis (*46*). In both yeast and mammalian cells, Bax-induced cell death involves dimerization, and targeting to mitochondrial membrane appears to be essential for Bax to exert a cytotoxic effect (*47*). Inducible expression of Bax in mammalian, yeast, and *E. coli* cells initiated cell death with generation of ROS, and a decrease in mitochondrial membrane potentials (*5*, *42*, *43*). Although our observation was taken as evidence that DED induced cell death in *E. coli*, it has close parallels with eukaryotic and mammalian systems (Figure 6C).

Overexpression of FADD-DED in the membranes of *E. coli* or exogenous treatment of *E. coli* cells along with the membrane component as a vehicle seems to generate ROS as seen in the antibiotic-mediated bacterial cell death or Bax-mediated apoptosis in mammalian cells. The use of proteomic tools to study protein expression change during FADD-DED-mediated bacterial cell death and validation by coexpression analysis provides a more complete picture of proteins involved in FADD-DED-induced cell death. This is important in understanding the molecular mechanism of FADD-DED-mediated cell death at the protein level. We illustrate that overexpression of FADD-DED in the membranes of *E. coli* actively downregulates the proteins of NADH generation, such as IDH. The differential expression of MDH, PckA, and PykF facilitates production of the antioxidant NADPH by the use of a pro-oxidant NADH. Coexpression of *E. coli* protein Hns involved in global growth arrest would help to overcome the lethal effect of FADD-DED. Our results provide a common mechanistic feature of cell death mediated by ROS, throughout prokaryotes and eukaryote.

ACKNOWLEDGMENT

We are grateful to Dr. M.-H. Yu for her help with the use of the facilities of the Functional Proteomics Center.

SUPPORTING INFORMATION AVAILABLE

SDS−PAGE analysis of *E. coli* proteins from coexpression studies with FADD-DED (Figure-S1), a list of PCR primers used for gene cloning in coexpression analysis (Table S1), a list of identified proteins from *E. coli* cells expressing FADD-DED (Table S2), mass spectrometric output for the proteins differentially expressed in this study (Table S3), and a list of selected *E. coli* proteins for coexpression with FADD-DED (Table S4). This material is available free of charge via the Internet at http://pubs.acs.org.

REFERENCES

1. Steller, H. (1995) Mechanisms and genes of cellular suicide. *Science 267*, 1445–1449.
2. Ameisen, J. C. (1996) The origin of programmed cell death. *Science 272*, 1278–1279.
3. Wheatley, D. N., Christensen, S. T., Schousboe, P., and Rasmussen, L. (1993) Signalling in cell growth and death: Adequate nutrition alone may not be sufficient for ciliates. A minireview. *Cell Biol. Int. 17*, 817–823.
4. Hochman, A. (1997) Programmed cell death in prokaryotes. *Crit. Rev. Microbiol. 23*, 207–214.
5. Asoh, S., Nishimaki, K., Nanbu-Wakao, R., and Ohta, S. (1998) A trace amount of the human pro-apoptotic factor Bax induces bacterial death accompanied by damage of DNA. *J. Biol. Chem. 273*, 11384–11391.
6. Lee, S. W., Ko, Y. G., Bang, S., Kim, K. S., and Kim, S. (2000) Death effector domain of a mammalian apoptosis mediator, FADD, induces bacterial cell death. *Mol. Microbiol. 35*, 1540–1549.
7. Zimmermann, K., Bonzon, C., and Green, D. (2001) The machinery of programmed cell death. *Pharmacol. Ther. 92*, 57–70.
8. Valmiki, M. G., and Ramos, J. W. (2009) Death effector domain-containing proteins. *Cell. Mol. Life Sci. 66*, 814–830.
9. Chinnaiyan, A. M., O'Rourke, K., Tewari, M., and Dixit, V. M. (1995) FADD, a novel death domain-containing protein, interacts with the death domain of Fas and initiates apoptosis. *Cell 81*, 505–512.
10. Kischkel, F. C., Hellbardt, S., Behrmann, I., Germer, M., Pawlita, M., Krammer, P. H., and Peter, M. E. (1995) Cytotoxicity-dependent APO-1 (Fas/CD95)-associated proteins form a death-inducing signaling complex (DISC) with the receptor. *EMBO J. 14*, 5579–5588.
11. Siegel, R. M., Martin, D. A., Zheng, L., Ng, S. Y., Bertin, J., Cohen, J., and Lenardo, M. J. (1998) Death-effector filaments: Novel cytoplasmic structures that recruit caspases and trigger apoptosis. *J. Cell Biol. 141*, 1243–1253.
12. Pandey, A., and Mann, M. (2000) Proteomics to study genes and genomes. *Nature 405*, 837–846.
13. Washburn, M. P., and Yates, J. R., III (2000) Analysis of the microbial proteome. *Curr. Opin. Microbiol. 3*, 292–297.
14. Henzel, W. J., Billeci, T. M., Stults, J. T., Wong, S. C., Grimley, C., and Watanabe, C. (1993) Identifying proteins from two-dimensional gels by molecular mass searching of peptide fragments in protein sequence databases. *Proc. Natl. Acad. Sci. U.S.A. 90*, 5011–5015.
15. Pappin, D. J., Hojrup, P., and Bleasby, A. J. (1993) Rapid identification of proteins by peptide-mass fingerprinting. *Curr. Biol. 3*, 327–332.
16. Blattner, F. R., Plunkett, G., III, Bloch, C. A., Perna, N. T., Burland, V., Riley, M., Collado-Vides, J., Glasner, J. D., Rode, C. K., Mayhew, G. F., Gregor, J., Davis, N. W., Kirkpatrick, H. A., Goeden, M. A., Rose, D. J., Mau, B., and Shao, Y. (1997) The complete genome sequence of *Escherichia coli* K-12. *Science 277*, 1453–1462.
17. Kim, H. J., Kang, H. J., Lee, H., Lee, S. T., Yu, M. H., Kim, H., and Lee, C. (2009) Identification of S100A8 and S100A9 as Serological Markers for Colorectal Cancer. *J. Proteome Res. 8*, 1368–1379.
18. Kim, D. H., Bae, J., Lee, J. W., Kim, S., Kim, Y. H., Bae, J. Y., Yi, J. K., Yu, M. H., Noh, D. Y., and Lee, C. (2009) Proteomic analysis of breast cancer tissue reveals upregulation of actin-remodeling proteins and its relevance to cancer invasiveness. *Proteomics: Clin. Appl. 3*, 30–40.
19. Gong, X., Fan, S., Bilderbeck, A., Li, M., Pang, H., and Tao, S. (2008) Comparative analysis of essential genes and nonessential genes in *Escherichia coli* K12. *Mol. Genet. Genomics 279*, 87–94.
20. Gomez-Angelats, M., and Cidlowski, J. A. (2003) Molecular evidence for the nuclear localization of FADD. *Cell Death Differ. 10*, 791–797.
21. Moody, C. S., and Hassan, H. M. (1982) Mutagenicity of oxygen free radicals. *Proc. Natl. Acad. Sci. U.S.A. 79*, 2855–2859.
22. Ames, B. N., and Gold, L. S. (1991) Endogenous mutagens and the causes of aging and cancer. *Mutat. Res. 250*, 3–16.
23. Kohanski, M. A., Dwyer, D. J., Wierzbowski, J., Cottarel, G., and Collins, J. J. (2008) Mistranslation of membrane proteins and two-component system activation trigger antibiotic-mediated cell death. *Cell 135*, 679–690.
24. Genova, M. L., Pich, M. M., Bernacchia, A., Bianchi, C., Biondi, A., Bovina, C., Falasca, A. I., Formiggini, G., Castelli, G. P., and Lenaz, G. (2004) The mitochondrial production of reactive oxygen species in relation to aging and pathology. *Ann. N.Y. Acad. Sci. 1011*, 86–100.
25. Cha, M. K., Kim, H. K., and Kim, I. H. (1995) Thioredoxin-linked "thiol peroxidase" from periplasmic space of *Escherichia coli*. *J. Biol. Chem. 270*, 28635–28641.
26. Cha, M. K., Kim, H. K., and Kim, I. H. (1996) Mutation and mutagenesis of thiol peroxidase of *Escherichia coli* and a new type of thiol peroxidase family. *J. Bacteriol. 178*, 5610–5614.
27. Nordberg, J., and Arner, E. S. (2001) Reactive oxygen species, antioxidants, and the mammalian thioredoxin system. *Free Radical Biol. Med. 31*, 1287–1312.
28. Singh, R., Lemire, J., Mailloux, R. J., and Appanna, V. D. (2008) A novel strategy involved anti-oxidative defense: The conversion of NADH into NADPH by a metabolic network. *PLoS One 3*, e2682.
29. Kohanski, M. A., Dwyer, D. J., Hayete, B., Lawrence, C. A., and Collins, J. J. (2007) A common mechanism of cellular death induced by bactericidal antibiotics. *Cell 130*, 797–810.
30. Dwyer, D. J., Kohanski, M. A., Hayete, B., and Collins, J. J. (2007) Gyrase inhibitors induce an oxidative damage cellular death pathway in *Escherichia coli*. *Mol. Syst. Biol. 3*, 91.
31. Bologna, F. P., Andreo, C. S., and Drincovich, M. F. (2007) *Escherichia coli* malic enzymes: Two isoforms with substantial differences in kinetic properties, metabolic regulation, and structure. *J. Bacteriol. 189*, 5937–5946.
32. Leist, M., Single, B., Castoldi, A. F., Kuhnle, S., and Nicotera, P. (1997) Intracellular adenosine triphosphate (ATP) concentration: A switch in the decision between apoptosis and necrosis. *J. Exp. Med. 185*, 1481–1486.

33. Dorman, C. J. (2004) H-NS: A universal regulator for a dynamic genome. *Nat. Rev. Microbiol. 2*, 391–400.
34. McGovern, V., Higgins, N. P., Chiz, R. S., and Jaworski, A. (1994) H-NS over-expression induces an artificial stationary phase by silencing global transcription. *Biochimie 76*, 1019–1029.
35. Imai, S., Armstrong, C. M., Kaeberlein, M., and Guarente, L. (2000) Transcriptional silencing and longevity protein Sir2 is an NAD-dependent histone deacetylase. *Nature 403*, 795–800.
36. Dukan, S., and Nystrom, T. (1998) Bacterial senescence: Stasis results in increased and differential oxidation of cytoplasmic proteins leading to developmental induction of the heat shock regulon. *Genes Dev. 12*, 3431–3441.
37. Dukan, S., and Nystrom, T. (1999) Oxidative stress defense and deterioration of growth-arrested *Escherichia coli* cells. *J. Biol. Chem. 274*, 26027–26032.
38. Scholz, C., Eckert, B., Hagn, F., Schaarschmidt, P., Balbach, J., and Schmid, F. X. (2006) SlyD proteins from different species exhibit high prolyl isomerase and chaperone activities. *Biochemistry 45*, 20–33.
39. Amici, A., Levine, R. L., Tsai, L., and Stadtman, E. R. (1989) Conversion of amino acid residues in proteins and amino acid homopolymers to carbonyl derivatives by metal-catalyzed oxidation reactions. *J. Biol. Chem. 264*, 3341–3346.
40. Levine, R. L., Moskovitz, J., and Stadtman, E. R. (2000) Oxidation of methionine in proteins: Roles in antioxidant defense and cellular regulation. *IUBMB Life 50*, 301–307.
41. Stadtman, E. R. (2004) Role of oxidant species in aging. *Curr. Med. Chem. 11*, 1105–1112.
42. Xiang, J., Chao, D. T., and Korsmeyer, S. J. (1996) BAX-induced cell death may not require interleukin 1 β-converting enzyme-like proteases. *Proc. Natl. Acad. Sci. U.S.A. 93*, 14559–14563.
43. Sato, T., Hanada, M., Bodrug, S., Irie, S., Iwama, N., Boise, L. H., Thompson, C. B., Golemis, E., Fong, L., and Wang, H. G.; et al. (1994) Interactions among members of the Bcl-2 protein family analyzed with a yeast two-hybrid system. *Proc. Natl. Acad. Sci. U.S.A. 91*, 9238–9242.
44. Greenhalf, W., Stephan, C., and Chaudhuri, B. (1996) Role of mitochondria and C-terminal membrane anchor of Bcl-2 in Bax induced growth arrest and mortality in *Saccharomyces cerevisiae*. *FEBS Lett. 380*, 169–175.
45. Jurgensmeier, J. M., Krajewski, S., Armstrong, R. C., Wilson, G. M., Oltersdorf, T., Fritz, L. C., Reed, J. C., and Ottilie, S. (1997) Bax- and Bak-induced cell death in the fission yeast *Schizosaccharomyces pombe*. *Mol. Biol. Cell 8*, 325–339.
46. Oltvai, Z. N., Milliman, C. L., and Korsmeyer, S. J. (1993) Bcl-2 heterodimerizes in vivo with a conserved homolog, Bax, that accelerates programmed cell death. *Cell 74*, 609–619.
47. Zha, H., Fisk, H. A., Yaffe, M. P., Mahajan, N., Herman, B., and Reed, J. C. (1996) Structure-function comparisons of the proapoptotic protein Bax in yeast and mammalian cells. *Mol. Cell. Biol. 16*, 6494–6508.